JOURNAL OF AIRCRAFT
Vol. 38, No. 4, July–August 2001

Optimization of Noise Abatement Departure Trajectories

H. G. Visser* and R. A. A. Wijnen†
Delft University of Technology, 2600 GB Delft, The Netherlands

Development is described of a new tool that offers significant capabilities for the analysis and design of noise abatement procedures at any given airport. The proposed tool combines a noise model, a geographic information system, and a dynamic trajectory optimization algorithm. The optimization algorithm essentially modifies routings and flight paths to minimize the noise impact in the residential communities surrounding the airport, while satisfying all imposed operational and safety constraints. Numerical examples, involving departure trajectories from Amsterdam Airport Schiphol, are included to demonstrate the effectiveness and flexibility of the developed tool. Although the results obtained to date are for departure flights only, the employed methodology tool holds out equal promise for application to approach trajectories. In the numerical examples the characteristics of the Boeing 737-300 aircraft are used.

I. Introduction

THE noise resulting from flight operations at major airports is a continuing source of annoyance in nearby residential communities. To mitigate the impact of aircraft noise, several operational measures have been adopted at some airports located close to sensitive communities. For example, at Amsterdam Airport Schiphol (AAS) in The Netherlands, the number of flight operations that can take place during a one-year period has been restricted. Noise abatement procedures have been adopted for both departure and approach flights.

Noise abatement procedures are designed to reduce noise exposure to the most sensitive areas in the vicinity of airports. A number of different noise abatement procedures have been proposed to date. The ICAO noise abatement departure, for example, is designed to minimize the total area impacted by aircraft noise, whereas thrust cutback departures have been developed to reduce the noise at specific locations.[1] The latter procedures may indeed result in a reduction in the area impacted by high-intensity noise, but this typically comes at the expense of an increased area of low-intensity noise. The true noise impact is dependent on the population density distribution in the vicinity of the airport.

Tools for developing noise abatement procedures are often based on the combination of a flight simulator, a noise model, and a geographic information system (GIS).[1] One of the most widely used tools for assessing the changes in noise impact resulting from revised routings or alternative flight paths is the Integrated Noise Model (INM).[2] INM has been the Federal Aviation Administration's standard methodology for noise impact assessment since 1978. Within INM, several noise metrics are available for evaluating aircraft noise. All of them are based on summation formulas, which start from single event contributions of individual aircraft flyovers, which are then summed for all aircraft operations from the airport. The noise impact is then presented in terms of the total area enclosed within the specified level contours for the selected noise metric. When the parameters that define the noise abatement procedures are systematically varied, the dimensions of the resulting noise contours can be eventually reduced.

The aim of the present study is to combine the INM, a GIS, and a dynamic trajectory optimization algorithm into a single tool that can be effectively used in the analysis and development of noise abatement procedures for both approach and departure. However, in the numerical examples only departures will be considered. The advantage of using trajectory optimization, rather than trajectory simulation, is that flight trajectories can be generated that are optimal in a user-defined sense in a very rapid and systematic fashion. To ensure that the noise abatement trajectories generated by this tool are flyable, practical, and effective, a trajectory optimization technique has been adopted that is capable of dealing with the large number of path constraints that result from operational requirements. Indeed, without the inclusion of these requirements, the danger exists that the resulting trajectories may be too complex to be flown in existing (IFR) guidance and navigation environments. It is expected that future guidance and navigation aids are likely to place less limitations on trajectories, primarily due to improvements in accuracy and coverage. The optimization tool proposed herein allows a quick and objective quantification of the potential noise benefits that may result from these advances in technology.

Clearly, noise impact is not the only environmental consideration used in the construction of a departure procedure. Air pollution and fuel-consumption considerations certainly are of concern as well. Improvements in noise impact can be typically achieved at the expense of an increased fuel consumption and, therefore, a compromise between these two conflicting requirements must be made. To permit such a tradeoff, a composite performance measure is used that consists of a weighted combination of a noise-related criterion and fuel consumed. To demonstrate the usefulness of the proposed trajectory optimization tool some numerical examples are presented that are based on a standard instrument departure currently in use at AAS, the so-called Spijkerboor departure.[3] The examples use the Boeing 737-300 twin-jet transport aircraft.

II. Problem Description

Among the quantities that are needed to define a trajectory optimization problem, perhaps the most important one is the performance index. The number of people within the exposed community that is expected to awake due to a single event nighttime noise intrusion has been used as the primary performance index in the present study. This particular performance index has the advantage that it offers a rather transparent measure for the true noise impact on the population living in the vicinity of the airport. However, in contrast to performance criteria that are based on the total area enclosed within specified noise level contours, the awakening criterion is site specific.

The specification of an awakening-related performance index requires knowledge of the relationship between aircraft noise and sleep disturbance. One such dose-response relationship was proposed by the Federal Interagency Committee on Aviation Noise (FICAN) in 1992.[4] This curve was largely based on studies of sleep disturbance that were primarily conducted in a laboratory environment. In 1997, FICAN revised the sleep disturbance relationship, based on new findings that were obtained through field studies, in which subjects were exposed to noise in their own homes. The new findings

Received 20 July 2000; revision received 16 February 2001; accepted for publication 17 February 2001.

*Lecturer, Faculty of Aerospace Engineering. Associate Fellow AIAA.
†Research Associate, Faculty of Aerospace Engineering. Member AIAA.

indicate that people are less likely to be awakened from sleep when the subjects are at home. The 1997 curve can be represented by the following relationship for the percentage of the exposed population expected to be awakened (% awakening) as a function of the exposure to single event noise levels expressed in terms of sound exposure level (SEL):

$$\%\text{awakenings} = 0.0087(\text{SEL}_{\text{ind}} - 30)^{1.97} \quad (1)$$

where SEL_{ind} is the sound exposure level (decibels) that occurs indoors. This relationship, shown in Fig. 1, has been used as the basis for determining the number of the awakenings. When the INM noise model is used, the noise contribution of an individual aircraft flyover can be computed in terms of the outdoor SEL. The indoor sound level is approximated in this study by lowering the computed outdoor level by 20.5 dB, which is a value that represents the average sound transmission loss for a home.

Additionally, when the distribution and density of the population in the residential communities near the airport is known, the absolute number of people that awake can be determined. In the present study, data of the population distribution around AAS, provided by the Dutch Directorate General of Civil Aviation, have been used to set up a GIS. This GIS is then used to calculate the number of people that awake due to flyover noise resulting from a Spijkerboor departure from runway 240 (see Fig. 2). In principle, a population distribution database corresponding to any given airport can be accommodated.

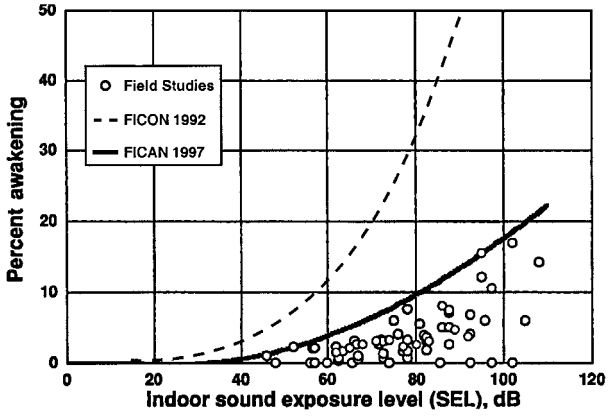

Fig. 1 FICAN proposed sleep disturbance dose-response relationship (from Ref. 4).

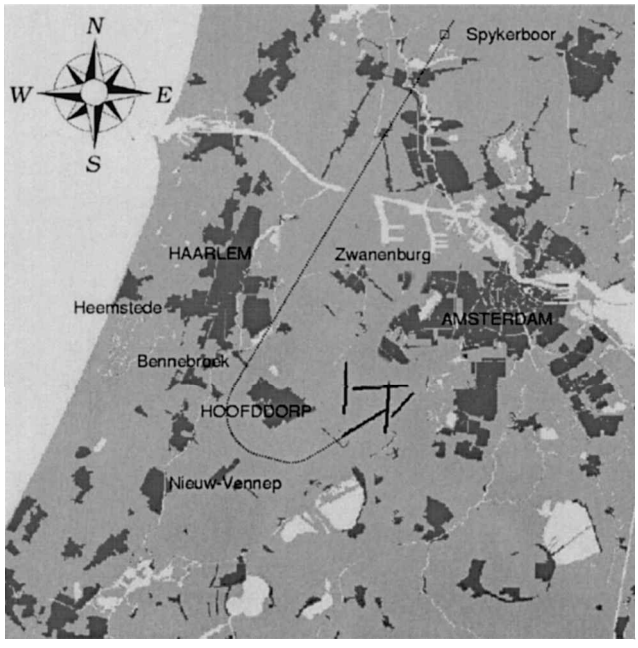

Fig. 2 Spijkerboor departure at AAS.

For SEL computations, observer locations are arranged in the form of a user-defined grid of points surrounding residential areas in the vicinity of the airport. The size and mesh of the grid has a significant impact on the computational burden. For this reason a rectangular grid of relatively modest dimensions (14×25 km) and with a relatively coarse mesh (1×1 km) has been defined for the Spijkerboor departure at AAS. To further alleviate the computational load, a noise calculation at a specific observer location is only performed if that location turns out to be populated.

To ensure an appropriate transition to and from en route flight conditions, the departure flight paths are computed for a specified range that extends well outside the noise-sensitive area. Because the computation of the noise impact is indeed confined to an area that is relatively small in comparison with the overall specified range, the secondary minimum-fuel objective in the composite performance index is crucial in shaping the terminal phase of the flight trajectories. Mathematically, the composite performance index can be expressed as

$$J = K \cdot \text{awakenings} + W_f \quad (2)$$

where W_f is the fuel consumed (in kilograms) and K a weighting factor. For moderate values of the weighting factor K, the utilization of this composite performance index typically results in fairly smooth minimum-fuel trajectories that are locally adjusted for noise considerations.

III. Acoustic Model

To evaluate aircraft flyover noise, a model has been developed that essentially implements the basic methodology employed by INM to compute the SEL at a given observer location.[2] The INM procedure for determining the SEL, at any specific location, is to select appropriate sound levels from a noise–thrust–distance (NTD) table corresponding to the distances from aircraft to observer. The NTD data contained in the INM database represent the noise exposure levels for specific reference conditions.

A very significant assumption on which the NTD database is based is that an aircraft proceeds along a straight line segment of infinite length. However, to model the movement of an aircraft in three-dimensional space, INM actually describes a flight path as a sequence of straight line segments of finite length. To obtain the noise level at an observer location due to an aircraft proceeding along a finite flight segment, the uncorrected NTD noise-level value must be adjusted by a fractional component. The SEL noise-fraction adjustment strongly depends on the geometry of the flight segment relative to the observer. In addition to the noise-fraction adjustment, a number of other adjustments have to be introduced to account for differences between the prevailing operational conditions and the reference conditions specified for the NTD tables. In this study, a speed adjustment (in decibels) and a lateral attenuation adjustment have been incorporated. The speed adjustment accounts for the aircraft's true airspeed deviating from the 160-kn reference value associated with the NTD data. The lateral attenuation adjustment allows for over-ground propagation effects on aircraft sound, including ground reflection effects, refraction effects, and airplane shielding effects.

To compute the SEL at a given observer point, the contribution of each segment of the flight path to the overall result has to be taken into account. In the trajectory optimizations it is assumed that a flight actually commences at an altitude of 122 m (400 ft). The run-up operation and takeoff flight path up to 122 m have not been considered. The reason for this omission is that these initial operations are simply not subject to optimization. If so desired, the noise contribution of a fixed flight path up to 122 m can be precomputed and added to the overall noise impact. Because the influence of the fixed initial path remains limited to the (unpopulated) vicinity of the runway, this particular correction has not been incorporated here.

IV. Flight-Path Computation

The flight-path computation methodology implemented in the INM package has not been adopted herein. A slightly simplified

point-mass model based on Ref. 5 has been used in the present study instead. The optimal trajectory calculations are based on the so-called intermediate model. The underlying assumption for the intermediate model is equilibrium of forces normal to the flight path. The implication of the simplifying assumption is that the aerodynamic drag is slightly underestimated in the sense that it is now evaluated as if the aircraft performs a quasi-linear flight. This particular model has been used extensively in studies concerning fuel-optimal trajectories, where it demonstrated an acceptable level of accuracy for a typical commercial aircraft.[5,6]

In the present calculations, performance data pertaining to the Boeing 737-300 aircraft are used. Only one aircraft weight ($m = 56{,}000$ kg) is considered in the calculations. Performance data for maximum takeoff thrust as well as maximum climb thrust are considered. Also drag polars for several flap settings are available. Because the flight trajectories commence at an altitude of 122 m (400 ft), the calculations have been performed with the undercarriage retracted.

V. Trajectory Optimization

In recent years, some very powerful direct numerical methods for the generation of optimal trajectories have become available. The direct approach relies on some form of discretizing of the problem formulation. The problem of choosing a control function is, thus, reduced to choosing a finite set of parameters. Nonlinear programming is then used to select the parameters such as to minimize a defined objective function. One of the most effective direct numerical methods for path-constrained trajectory optimization is the collocation method.[6,7] Collocation involves discretization of the trajectory dynamics. The discrete dynamics along with the path constraints are then treated as algebraic inequalities to be satisfied by the nonlinear program (implicit integration). A major advantage of the direct optimization approach is that, unlike indirect (variational) methods, there is generally little difficulty in imposing constraints along the flight path. However, for the problem at hand the main advantage of this approach lies in that the collocation discretization is fully compatible with the discretization (segmentation) approach taken in the INM model.

In this study the recently developed EZopt[‡] program has been used to perform the optimal trajectory calculations. This program, which implements a simple variant of the collocation method, proved to be ideally suited for this problem, especially because it turned out to be quite capable in dealing with so-called multiphase trajectory optimization problems. Occasionally, discontinuities may occur in the dynamic system equations describing the motion of the aircraft. Such discontinuities tend to result in significant problems in the optimization process. When a multiphase formulation is resorted to, these problems can be overcome. A multiphase formulation allows discontinuities at phase transitions, as well as the implementation of different dynamic systems for different phases. The multiphase feature of EZopt is of vital importance for the noise-optimization procedure proposed herein because system discontinuities do indeed occur due to changes in flap setting and thrust rating.

The collocation discretization used in EZopt transforms the state and control functions to a set of discrete variables by subdividing each flight phase into a number of segments. The selection of the number and length of segments typically represents a tradeoff between the desired accuracy level of the numerical solution and the allowable computational burden. In the present optimal noise abatement study, the flight-path segmentation has been primarily based on the requirements associated with the computational methodology employed in the INM model.

VI. Departure Scenarios

A. Description of Spijkerboor Departure

To examine the usefulness of the trajectory optimization algorithm, some numerical experiments have been conducted for departure flights from AAS. The Spijkerboor departure has been selected as the baseline scenario, primarily because it represents a fairly noise-sensitive route. As shown in Fig. 2, the Spijkerboor departure involves a right turn shortly after lifting off from runway 240. A close inspection of Fig. 2 shows that an aircraft has to maneuver between the two residential areas, Hoofddorp (57,000 inhabitants) and Nieuw–Vennep (15,000 inhabitants). The right turn is followed by an interception of radial 213 of the Spijkerboor VOR. This particular route brings an aircraft fairly close to the communities of Bennebroek (5,000 inhabitants), Heemstede (26,000 inhabitants), and Haarlem (150,000 inhabitants). Moreover, on the other side of the flight track, Zwanenburg (8,000 inhabitants) is exposed to noise to a significant extent.

B. Multiphase Formulation

For a realistic representation of an optimized departure trajectory from runway 240 to the Spijkerboor VOR, the actual flight path is split up into four sequential phases. In the first phase, the aircraft flies a straight flight path starting at 122-m (400-ft) altitude and 90-m/s indicated airspeed (IAS), executed with a maximum takeoff thrust rating and flap setting 1. The first phase terminates when the indicated airspeed reaches the flaps retraction speed (100 m/s). The second phase is similar to the first phase except that it is now flown in a clean configuration. The second phase terminates when an altitude of 457 m (1500 ft) is reached and the maximum thrust rating is reduced to the maximum climb setting. In the third and subsequent phases turning is permitted. Also, a speed restriction is enforced in the third phase. The third phase ends when an altitude of 3048 m (10,000 ft) is reached. The final (fourth) phase is similar to the third phase except that the speed restriction is no longer applicable. The final phase terminates at an altitude of 4500 m.

C. Boundary and Staging Conditions

The equations of motion are written here in a coordinate frame fixed in space that has its origin at the grid point closest to the initial point of the departure trajectory. This initial point is located on the runway centerline extension, some 2800 m from the threshold of runway 240.

To ensure a flight of sufficient long duration, the endpoint of the flight trajectory is not located at the Spijkerboor VOR, but rather at some point well beyond it. All components of the final state vector have been specified, primarily to ensure that noise abatement does not result in unrealistic behavior in the terminal flight phase. The specified final altitude is 4500 m, and the required terminal speed is 275-kn IAS. These values have been selected based on earlier minimum-fuel studies. The final value for the heading angle is specified as 33 deg to allow the final stage of the flight to conform with the existing Spijkerboor departure, that is, flying along radial 213 inbound to Spijkerboor VOR. To enable thrust cutbacks, the flight time has not been specified in the examined scenarios.

In a multiphase formulation so-called staging (or phasing) conditions need to be included. Staging conditions are constraints that specify how the state at the end of a particular phase corresponds to the initial state in a subsequent phase. In the present formulation, the staging conditions are quite simple in the sense that the initial state of a particular phase is directly and fully connected to the terminal state of the preceding phase.

D. Operational Constraints

A variety of constraints needs to be imposed in any given scenario. These constraints arise as a result of existing operational requirements and also ensure that the trajectories generated by the optimization tool remain practically feasible and more or less resemble the flight paths that are currently flown.

The usual constraints include a limit for the aerodynamic roll angle μ, which is limited by

$$|\mu| \leq \mu_{\max} \tag{3}$$

The results presented in this study are based on a roll-angle limit of 25 deg, unless explicitly indicated otherwise.

[‡] Data available online at http://www.ama-inc.com.

Some operational speed limits also need to be obeyed. Particularly notable is the air traffic control imposed speed constraint of 250-kn IAS on climb-out paths, below 10,000-ft altitude:

$$\text{IAS} \leq 250 \text{ kn} \tag{4}$$

For the existing Spijkerboor departure, additional speed constraints are in effect, in the sense that during the right turn the indicated airspeed must be less than 220-kn IAS. The latter constraint has also been included in the trajectory optimization formulation. However, in some examples only the constraint given by Eq. (4) has been taken into account.

The minimum-fuel trajectories study presented in Refs. 6 and 8 revealed that to obtain realistic results additional path constraints need to be included to inhibit (local) loss of speed (IAS) and altitude h during a departure flight. To preclude these phenomena, two simple constraints are added to the problem formulation, namely,

$$\frac{\mathrm{d}h}{\mathrm{d}t} \geq 0, \qquad \frac{\mathrm{d(IAS)}}{\mathrm{d}t} \geq 0 \tag{5}$$

Note that as a result of the constraints (5), specific energy, that is, the sum of kinetic and potential energies, can never decrease as the flight progresses.

Some care has to be taken in the formulation of the thrust constraints. The application of thrust cutback should be compatible with aircraft performance to the extent that the engine-out climb gradient can be maintained after engine failure and subsequent thrust restoration. The application of reduced thrust should thus depend on the aircraft gross weight. Performance-related thrust constraints have, as yet, not been considered. The simple approach taken is to enforce a constraint on the relative thrust:

$$0.6 \leq T/T_{\max} \leq 1 \tag{6}$$

In other words, the thrust level can not be reduced below 60% of the maximum value. A more detailed study involving the influence of more realistic thrust constraints on the optimal noise-abatement procedures is envisaged for the near future.

Finally, some geometric constraints have been introduced that are needed to ensure that noise-optimized tracks exit the noise-observer grid area at an appropriate location. The geometric constraints can be removed if the grid is enlarged to the extent that the entire trajectory is contained within it.

VII. Numerical Examples

A. Baseline Results

To investigate the characteristic features of the optimal departure trajectories, the principal parameters that have been varied are the weighting factor of the performance index, the speed limit, and the roll-angle limit. The reference situation that has been selected here concerns a full-thrust, fuel-optimal departure (weighting factor $K = 0$), a roll-angle limit of 25 deg, and a 220-kn speed limit below 10,000 ft altitude.

In Fig. 3, some key results pertaining to the baseline scenario are shown. Figures 3 show the aircraft departure flight path in three-dimensional space, along with the projection of the flight path onto the horizontal plane (ground tracks). Note that only the initial part of the overall flight trajectory is shown. In addition to the flight path, also the noise grid and a contour plot associated with a key metric is shown in each of the four graphs. The four selected metrics are, respectively, outdoor SEL, the percentage of people expected to awake (per square kilometer), the population density distribution, and the number of people awakened as a result of the flyover.

Figure 4 shows similar results for a noise-optimized trajectory. This particular trajectory will be referred to as the minimum-noise trajectory, although strictly speaking this is not correct. The noise-optimized trajectory has actually been computed with the weighting factor K in the performance index set to 0.01. This implies that the defined minimum-noise trajectory is to a large extent still shaped by fuel considerations. Because the value 0.01 is the largest value that has been considered for the weighting factor K, the corresponding

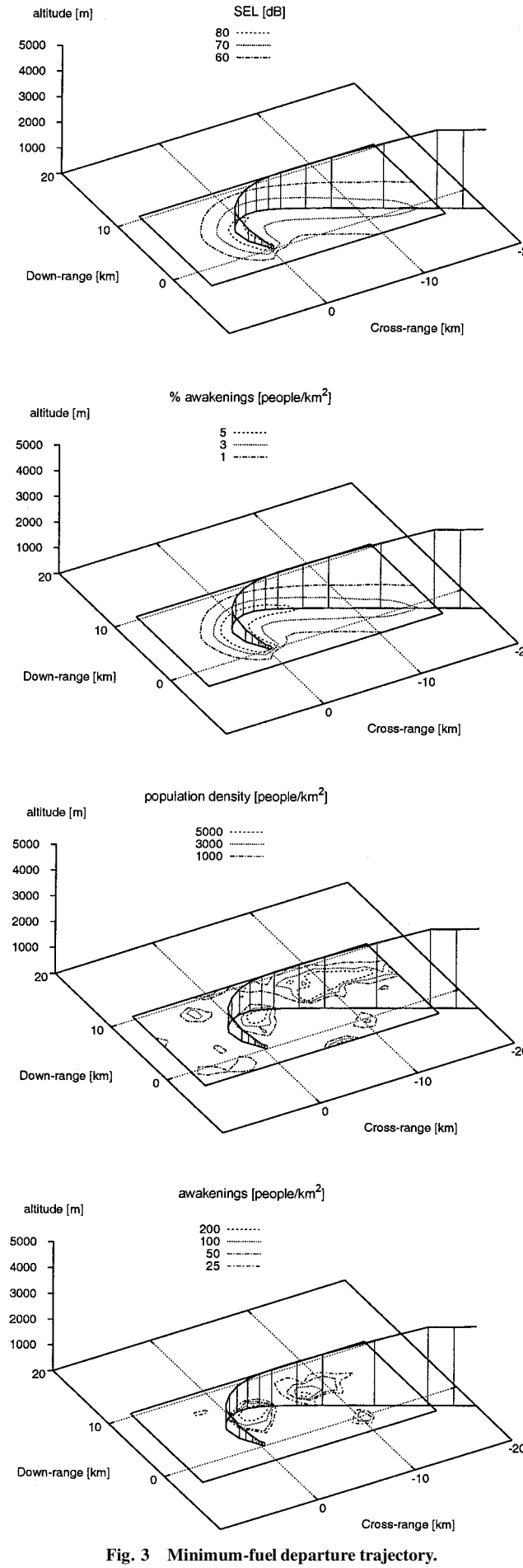

Fig. 3 Minimum-fuel departure trajectory.

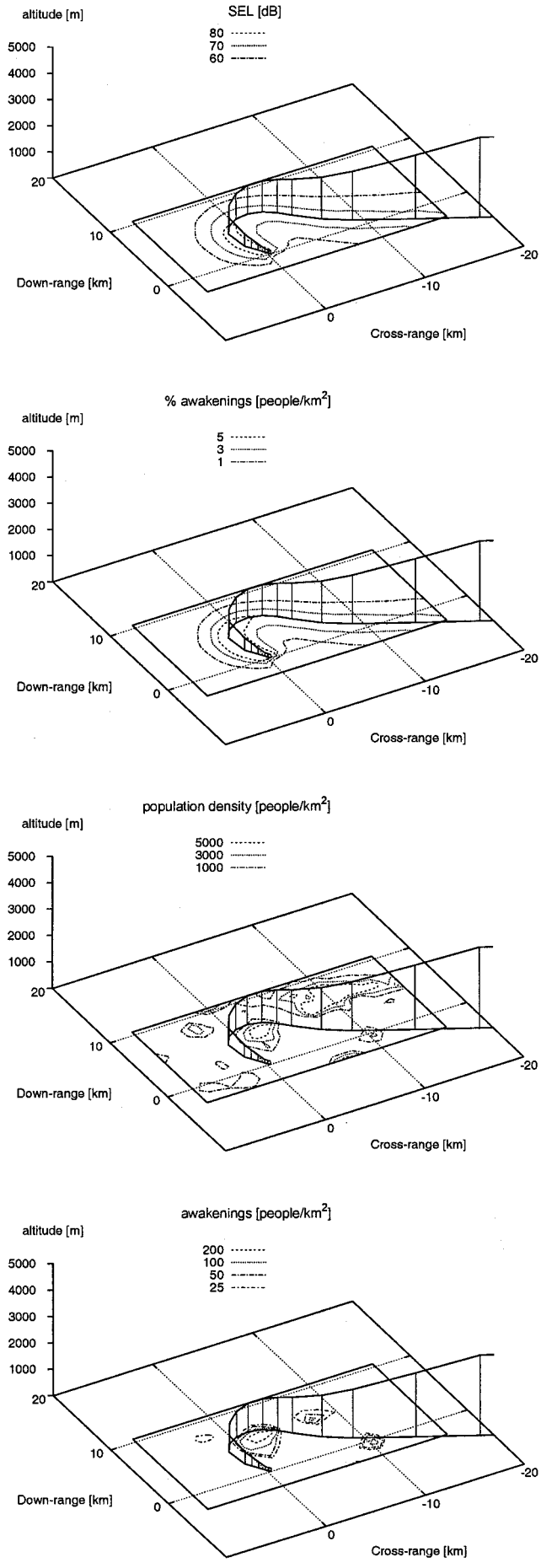

Fig. 4 Minimum-noise departure trajectory.

trajectory offers relatively the best performance in terms of awakenings among the results presented here.

To examine the characteristics of the optimized trajectories, it is of interest to compare the minimum-fuel and minimum-noise trajectories presented in Figs. 3 and 4. First, it is readily clear that for the fuel-optimal trajectory the 80-dB noise contour is somewhat larger, whereas the 70-dB noise contour is actually substantially smaller than for the minimum-noise trajectory. As a matter of fact, the 70-dB contour is completely contained within the noise grid only for the minimum-fuel case. Apparently, improvements in noise performance in the proximity of the departure runway come to a certain extent at the expense of the noise performance in more distant regions. Not surprisingly, the percent awakening contours are very similar in shape to the SEL contours. As has been pointed out before, the true noise impact heavily depends on the actual population distribution. A close inspection of the results shows that, especially in the vicinity of the city of Haarlem, the noise impact can be significantly reduced in a noise-optimal trajectory. However, in the relatively small community of Zwanenburg, the noise exposure is actually somewhat increased. This is because the noise-optimal trajectory now directly overflies Zwanenburg. Nevertheless, the overall improvements in noise impact that can be obtained are fairly impressive for the considered scenario. Indeed, the number of people that awake due to noise impact reduces from 5042 for the fuel-optimal trajectory to 3312 for the noise-optimal trajectory. In other words, a reduction of nearly 35%. The total population living within the area defined by the noise grid is 371,635. Consequently, the reduction in awakenings in relative terms is from approximately 1.4% to about 0.9%. With respect to fuel consumption, the differences between the minimum-fuel and the minimum-noise trajectories are rather modest. The noise-optimal trajectory requires only about 1% more fuel.

To illustrate how the improvements in noise performance are brought about, some more detailed trajectory optimization results are shown in Fig. 5. The first two phases (flown with maximum takeoff thrust) are actually the same for the two trajectories. In the first phase, the aircraft accelerates horizontally to the flap retraction speed. In the second phase, the aircraft climbs at a constant airspeed up to 457 m (1500 ft) above airport elevation. In the subsequent third phase, some major differences in controlling the flight path arise. Recall that in this phase a full-bank right turn takes place. Unlike in the minimum-noise trajectory, the climb at constant airspeed is initially maintained in the third phase of the minimum-fuel flight path. At an altitude of about 720 m, the minimum-fuel trajectory features a horizontal transition segment during which the aircraft accelerates to the 220-kn IAS limit. Such a low-altitude horizontal turn is actually a fairly typical feature for minimum-fuel trajectories.[6,8] It is evident, however, that from a noise perspective a horizontal turn at low altitude, executed at full thrust, is less desirable.

In the noise-optimal trajectory, the aircraft transitions much earlier to the 220-kn IAS limit. To this end, the climb rate is reduced, and full thrust is maintained. As expected, no low-altitude horizontal flight segment is present in the noise-optimal solution. A thrust cutback takes place when the aircraft overflies the westside of Hoofddorp. The thrust cutback is actually the main instrument to reduce the noise impact in this area. Also Heemstede and Haarlem benefit from the thrust cutback. Moreover, the noise impact in the two latter cities is favorably influenced by the slightly extended right turn, followed by a modest left turn. This particular behavior allows the noise impact to be shifted from densely populated city areas to the more rural regions.

When the value of the weighting factor K in increased Eq. (2), the minimum-fuel problem can be gradually moved to a minimum-noise formulation. When the value of K is increased, the extent of the thrust cutbacks is increased. Clearly, there are limitations to the extent of the thrust cutback that can be sustained for any given set of boundary conditions. In the present study, it turns out that the weighting factor K can not be taken significantly larger than 0.01. Figure 6 shows the optimal noise and fuel performance for a range of values of the weighting factor. The presented results are for scenarios that are similar to the baseline scenario, except that the 220-kn IAS

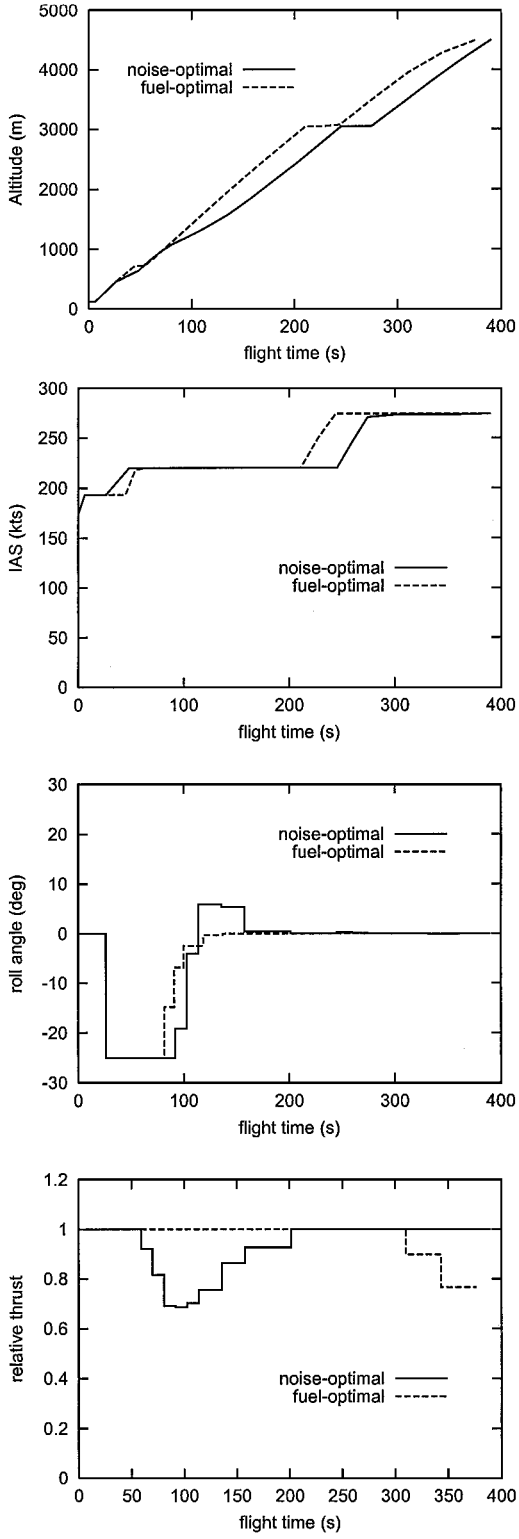

Fig. 5 Comparison of minimum-fuel and minimum-noise departure trajectories.

constraint has not been enforced. The corresponding results for the speed-constrained cases are quite similar though. As expected, the number of awakenings sharply decreases as the weighting factor K increases. The fuel penalty resulting from the thrust cutbacks remains quite modest.

B. Assessing the Speed Constraint

In the scenarios presented in the preceding section, the 220-kn IAS constraint that is currently enforced in the Spijkerboor departure

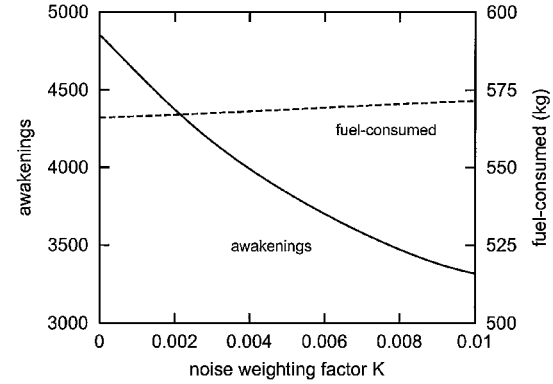

Fig. 6 Comparison of optimal performances for various values of weighting factor K.

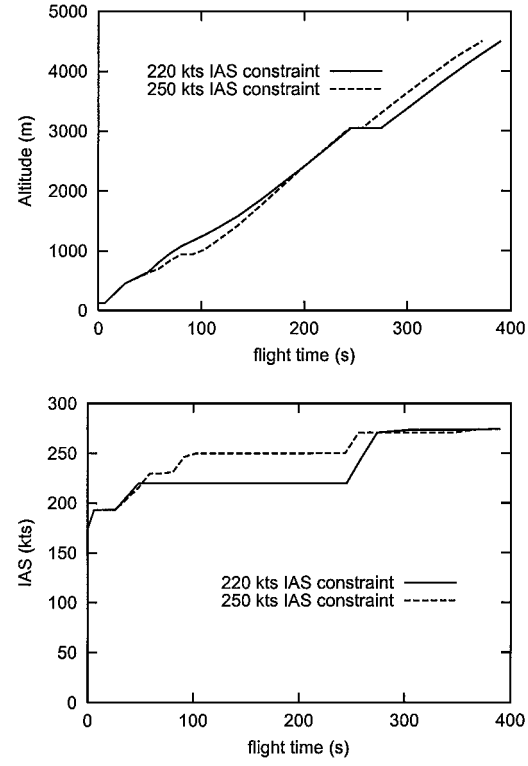

Fig. 7 Minimum-noise departure trajectories for two speed limits.

has been retained. To assess the impact of the speed constraint on the optimal performance, a noise-optimal-departure trajectory has been computed for the less restrictive 250-kn IAS speed limit. Figure 7 compares the time histories for altitude and speed for the two speed-limited cases ($K = 0.01$). Somewhat surprisingly, the horizontal turn segment reemerges in the noise-optimal trajectory corresponding to the 250-kn IAS constraint, albeit at a slightly higher altitude than in the fuel-optimal solution (see Fig. 5). Apparently, the added freedom to optimize is utilized to improve the fuel performance rather than the noise performance. Indeed, the number of people that awake is hardly affected, but the fuel consumption is reduced by some 12 kg (or 2%).

C. Assessing the Roll-Angle Constraint

One of the most surprising features of the minimum-noise trajectory presented in Fig. 4 is that, in the right turn, the densely populated westside of Hoofddorp is overflown. One would suspect that a less tight turn would actually be more favorable in terms of noise impact in this particular situation. To examine whether this

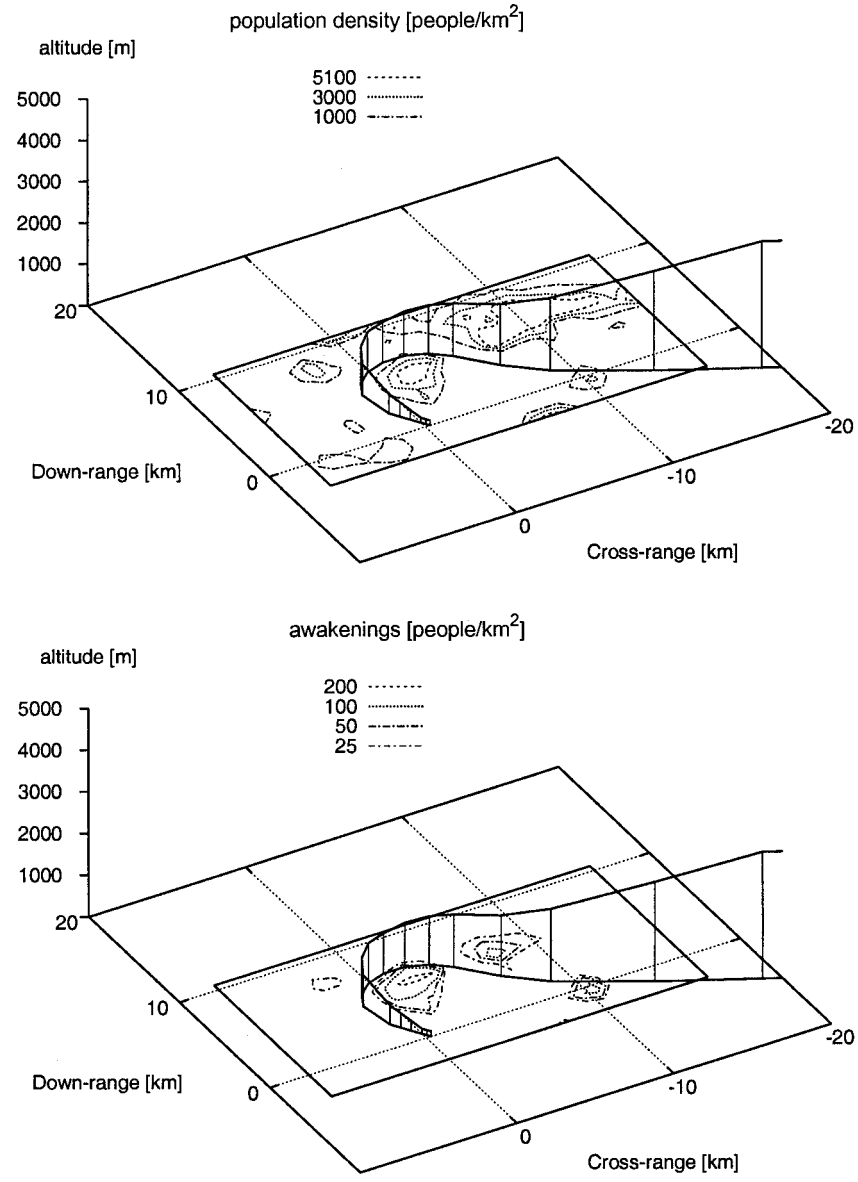

Fig. 8 Minimum-noise departure trajectory for a reduced roll-angle limit (20 deg).

is indeed the case, a noise-optimal trajectory has been evaluated with the aerodynamic roll-angle limit reduced to 20 deg. Figure 8 shows that a wider turn does indeed result in a reduction of the noise impact in the Hoofddorp area. The downside of this wider turn is that the number of people that awake in the cities of Heemstede and Haarlem is substantially increased. On balance, the total number of awakenings is in fact slightly increased from 3312 to 3325. More significantly, the wider turn results in an increase of fuel consumption of about 12 kg (or 2%).

VIII. Conclusions

A numerical tool for calculating noise-optimized departure trajectories has been developed by using a collocation trajectory optimization technique in conjunction with the noise model derived from the INM program. The essential feature of the proposed approach is that the flight-path segmentation employed by the trajectory optimization technique is fully compatible with the segmentation approach adopted in the INM noise model. The proposed trajectory optimization tool supports multiphase formulations and readily allows the inclusion of multiple flight-path constraints. The latter feature is particularly important to enable the imposition of any safety standard or user requirement.

The present study is limited in scope in the sense that extensive parametric investigations have not taken place yet. Only a single departure route and a single aircraft type have been considered. Important parameters that need to be examined in future research include takeoff weight, wind, and off-nominal atmospheric conditions. As yet, only departure trajectories have been examined, but research efforts are currently underway to examine the applicability of the tool to approach trajectories as well.

The developed optimization concept is generic and flexible in the sense that alternative optimization criteria (e.g., noise-contour related criteria), additional constraints (e.g., restrictions resulting from navigation aids, safety requirements), or model refinements (e.g., a dynamic model featuring additional degrees of freedom) can be readily introduced.

In follow-on studies, the tool needs to be evaluated thoroughly via detailed parametric studies and applications to a variety of flight procedures currently in use. Also, the sensitivity of the solutions with respect to the size and mesh of the noise grid needs to be examined. However, on the indication of the results obtained thus far the developed noise-abatement trajectory optimization tool appears to hold out great promise for the design of new noise-abatement procedures.

Acknowledgments

We would like to thank Ton Kolijn of the Rijksluchtvaartdienst, Eric Koomen of the Rijkswaterstaat Meetkundige Dienst, Michiel

Cappendijk of Bridgis, and Peter Nieland of Kadata, for kindly supplying the population density distribution data for the area surrounding Amsterdam Airport Schiphol.

References

[1]Clarke, J.-P., and Hansman, R. J., "Systems Analysis of Noise Abatement Procedures Enabled by Advanced Flight Guidance Technology," AIAA Paper 97-0490, Jan. 1997.

[2]Office of Environment and Energy, "Integrated Noise Model (INM) Version 5.1 Technical Manual," Rept. FAA-AEE-97-04, Federal Aviation Agency, Dec. 1997.

[3]Air Traffic Control, The Netherlands, "Aeronautical Information Publication Netherlands," Rept. EHAM AD 2-2-7.43C, Schiphol Airport, The Netherlands, 11 Feb. 1999.

[4]"Sleep Disturbance Caused by Aviation Noise," Federal Interagency Committee on Aviation Noise (FICAN), March 1997.

[5]Wijnen, R. A. A., "Simulation and Optimization of Take-off Procedures for Noise Abatement," M.Sc. Thesis, Faculty of Aerospace Engineering, Delft Univ. of Technology, Delft, The Netherlands, Aug. 1998.

[6]Visser, H. G., "A 4-D Trajectory Optimization and Guidance Technique for Terminal Area Traffic Management," Rept. LR-769, Faculty of Aerospace Engineering, Delft Univ. of Technology, Delft, The Netherlands, June 1994.

[7]Hargraves, C. R., and Paris, S. W., "Direct Trajectory Optimization Using Nonlinear Programming and Collocation," *Journal of Guidance, Control, and Dynamics*, Vol. 10, No. 4, 1987, pp. 338–342.

[8]Visser, H. G., "Four-Dimensional Fuel Optimal Flights into and out of the Terminal Area," *Proceedings of the 17th International Congress on Aeronautical Sciences Congress*, Stockholm, 1990, pp. 1468–1478.